Electronic Supplementary Information

Quantitative Encapsulation and Retention of ^{227}Th and Decay Daughters in Core–Shell Lanthanum Phosphate Nanoparticles

M. Toro-González[1,2](✉), A. N. Dame[2], C. M. Foster[3], L. J. Millet[4], J. D. Woodward[2], J. V. Rojas[1], S. Mirzadeh[2], S. M. Davern[2](✉)

[1] Department of Mechanical and Nuclear Engineering, Virginia Commonwealth University, Richmond 23284, USA
[2] Isotope and Fuel Cycle Technology Division, Oak Ridge National Laboratory, Oak Ridge 37830, USA
[3] Biosciences Division, Oak Ridge National Laboratory, Oak Ridge 37830, USA
[4] Biosciences Division, Oak Ridge National Laboratory, Oak Ridge 37830, USA; Joint Research Activity, The Bredesen Center, University of Tennessee, Knoxville 37996, USA

ORCID: 0000-0003-3320-423X (M. Toro-González), 0000-0002-9577-5006 (A. N. Dame), 0000-0001-6443-2505 (L. J. Millet), 0000-0002-2268-4613 (J. V. Rojas), 0000-0002-1774-7958 (S. Mirzadeh), 0000-0003-2755-8912 (S. M. Davern)

Address correspondence to M. Toro-González (torogonzalezm@vcu.edu, torogonzalmt@ornl.gov) and S. M. Davern (davernsm@ornl.gov)

Table S1 Decrease in pH after synthesis of $LaPO_4$ C NPs. Summary of pH from $LaCl_3$-$Na_5P_3O_{10}$ mixture, as-prepared and dialyzed $LaPO_4$ C NPs suspensions synthesized using different procedures.

Procedure	pH		
	$LaCl_3$-$Na_5P_3O_{10}$ mixture	$LaPO_4$ C NPs as-prepared	$LaPO_4$ C NPs dialyzed
A	6.4	4.7	5.8
B	8.0	6.4	Not measured
C	8.1	7.1	Not measured

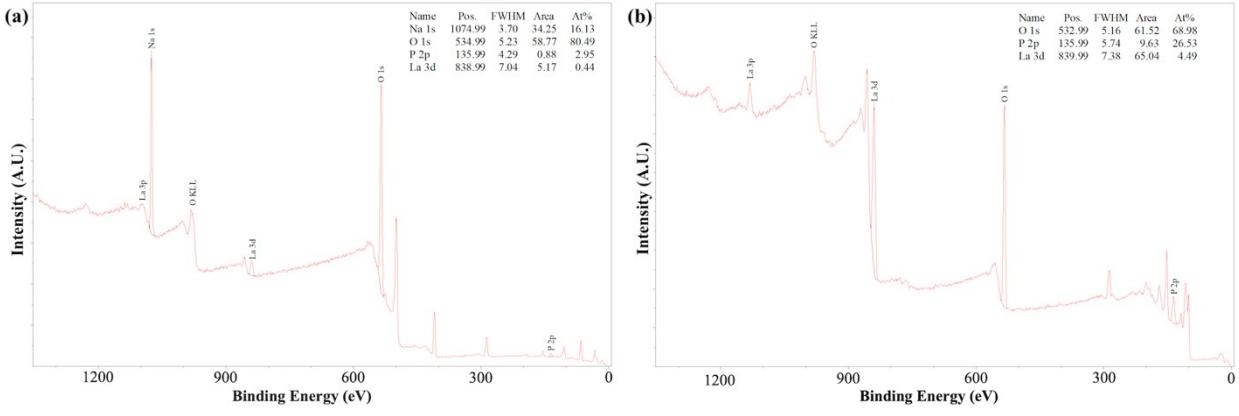

Fig. S1 Decrease in atomic fraction of sodium cations after dialysis of $LaPO_4$ C NPs. Representative X-ray photoelectron survey spectra of $LaPO_4$ C NPs (a) before and (b) after dialysis. Characteristic Na 1s, O 1s, P 2p, and La 3d electron transitions were observed in the survey spectra of $LaPO_4$ C NPs. The O KLL peak represents the energy of the electrons ejected from the O atoms due to the filling of the O 1s state (K-shell) by an electron from the L-shell coupled with the ejection of an electron from the L-shell. These results showed that there is a significant fraction of sodium cations originating from the reagents, which precipitated after synthesis and that are completely removed during dialysis of the NP suspension.

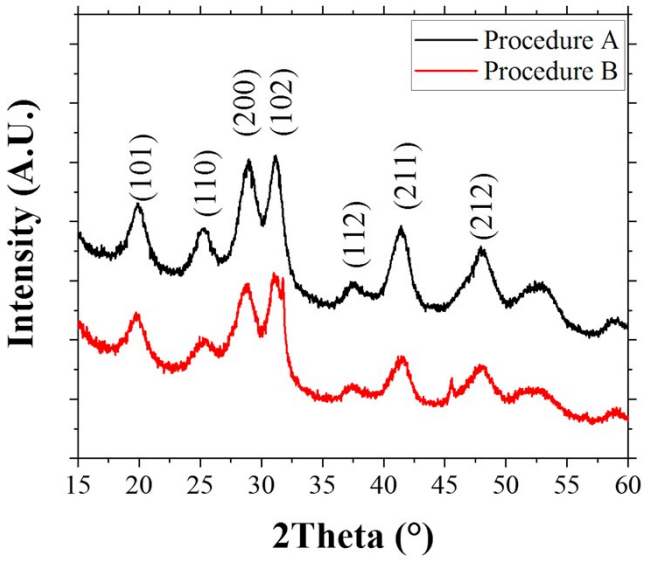

Fig. S2 Similar crystal structure and crystallite size of $LaPO_4$ C NPs increasing the concentration of $Na_5P_3O_{10}$. Diffraction patterns of $LaPO_4$ C NPs synthesized following procedures A and B. $LaPO_4$ C NPs are characterized with a hexagonal crystal system having a space group $P6_222$ (powder diffraction file: 01-075-1881). A crystallite size of 4.1 ± 0.5 nm and 4.0 ± 1.1 nm was obtained for $LaPO_4$ C NPs synthesized following procedures A and B, respectively.

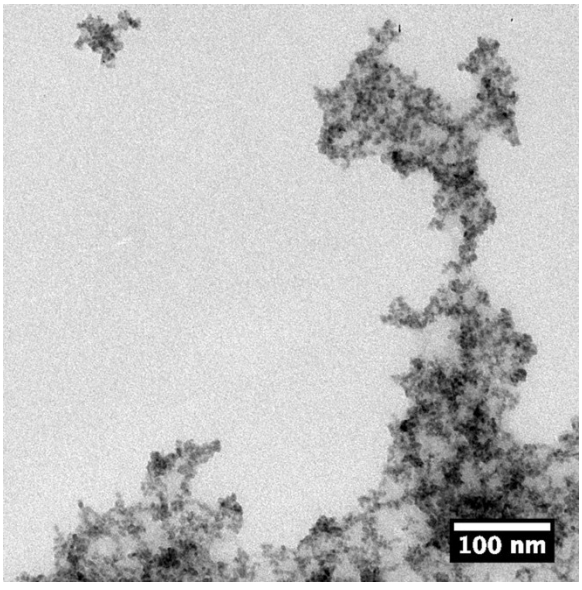

Fig. S3 Spherical and ellipsoidal $LaPO_4$ C NPs having a particle size below 10 nm. Micrograph of $LaPO_4$ C NPs synthesized following procedure C.

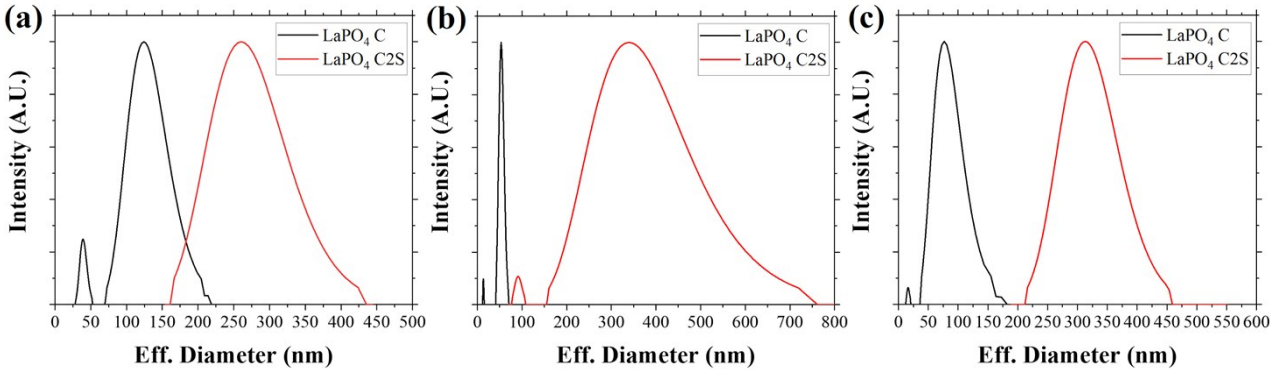

Fig. S4 Increase in effective diameter after deposition of two nonradioactive $LaPO_4$ shells onto $LaPO_4$ C NPs. Representative size distribution of $LaPO_4$ C and C2S NPs synthesized following procedure (a) A, (b) B, and (c) C. NP suspensions synthesized using procedures A and B were diluted 100 times in phosphate buffered saline (1X, pH 7.2), while a 10 times dilution was used for samples prepared following procedure C. All NP suspensions were filtered using a 0.2 µm Supor® Membrane filter before characterization.

Table S2 Increase in effective diameter and polydispersity index after deposition of two nonradioactive $LaPO_4$ shells onto $LaPO_4$ C NPs. Effective diameter size, polydispersity index, and zeta potential of $LaPO_4$ C and C2S NPs synthesized following different procedures.

Procedure	Sample	Effective diameter (nm)	Polydispersity index	Zeta potential (mV)
A	$LaPO_4$ C	96.8 ± 2.0	0.166 ± 0.027	−22.4 ± 2.0
	$LaPO_4$ C2S	264.6 ± 15.5	0.185 ± 0.033	−15.0 ± 2.5
B	$LaPO_4$ C	46.6 ± 0.6	0.150 ± 0.009	−14.3 ± 2.1
	$LaPO_4$ C2S	298.4 ± 29.6	0.167 ± 0.015	−10.4 ± 2.8
C	$LaPO_4$ C	73.9 ± 1.4	0.184 ± 0.014	−25.1 ± 5.1
	$LaPO_4$ C2S	255.2 ± 18.5	0.371 ± 0.045	−23.4 ± 2.9

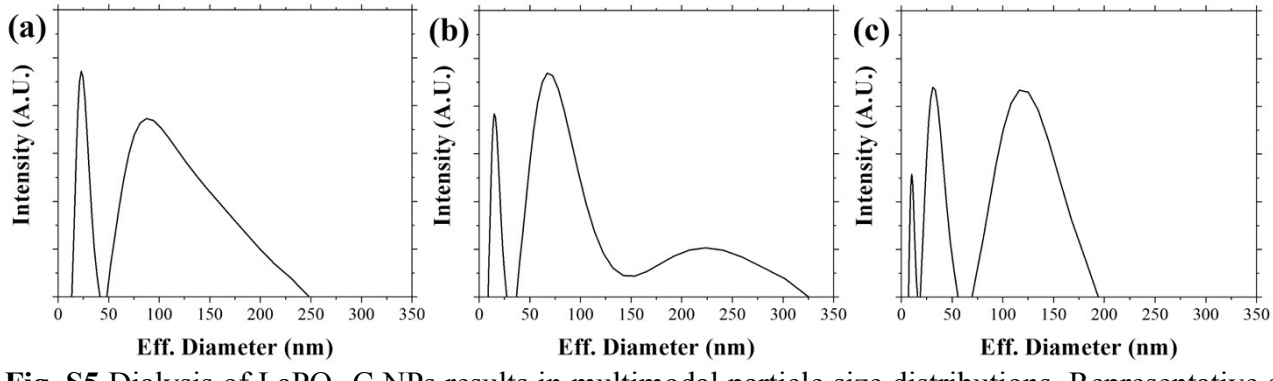

Fig. S5 Dialysis of $LaPO_4$ C NPs results in multimodal particle size distributions. Representative size distributions of $LaPO_4$ C NPs synthesized following procedure A, after dialysis at pH of (a) 5.7, (b) 8.8, and (c) 10 for 72 h. NP suspensions were characterized without adjusting the pH or the sample concentration. All NP suspensions were filtered using a 0.2 µm Supor® Membrane filter before characterization.

Table S3 Alkaline conditions during dialysis resulted in an increase of the effective diameter and polydispersity index of $LaPO_4$ C NPs. Effective diameter, polydispersity index, and zeta potential of $LaPO_4$ C NPs, synthesized following procedure A, after dialysis at different pH for 72 h.

Dialysate pH	Effective diameter (nm)	Polydispersity index	Zeta potential (mV)
10	257.2 ± 80.1	0.190 ± 0.050	−34.2 ± 2.0
8.8	140.9 ± 23.2	0.114 ± 0.016	−35.4 ± 4.0
5.7	130.5 ± 13.8	0.104 ± 0.013	−35.0 ± 2.0
3.5	Not measured	Not measured	0.4 ± 0.4

Note: the effective diameter and polydispersity index of $LaPO_4$ C NPs dialyzed at a pH of 3.5 were not measured because the particles are not stable and readily precipitate under the dialyzed conditions.

Table S4 Decrease in $LaPO_4$ C NPs concentration shifts the zeta potential to less negative values. Zeta potential of $LaPO_4$ C NPs synthesized following Procedure A at different concentrations.

Concentration (µg/mL)	Zeta potential (mV)
1,000	−43.7 ± 0.4
500	−47.7 ± 0.9
250	−46.1 ± 1.0
50	−35.2 ± 0.6
10	−24.3 ± 2.5
2	−9.4 ± 2.7

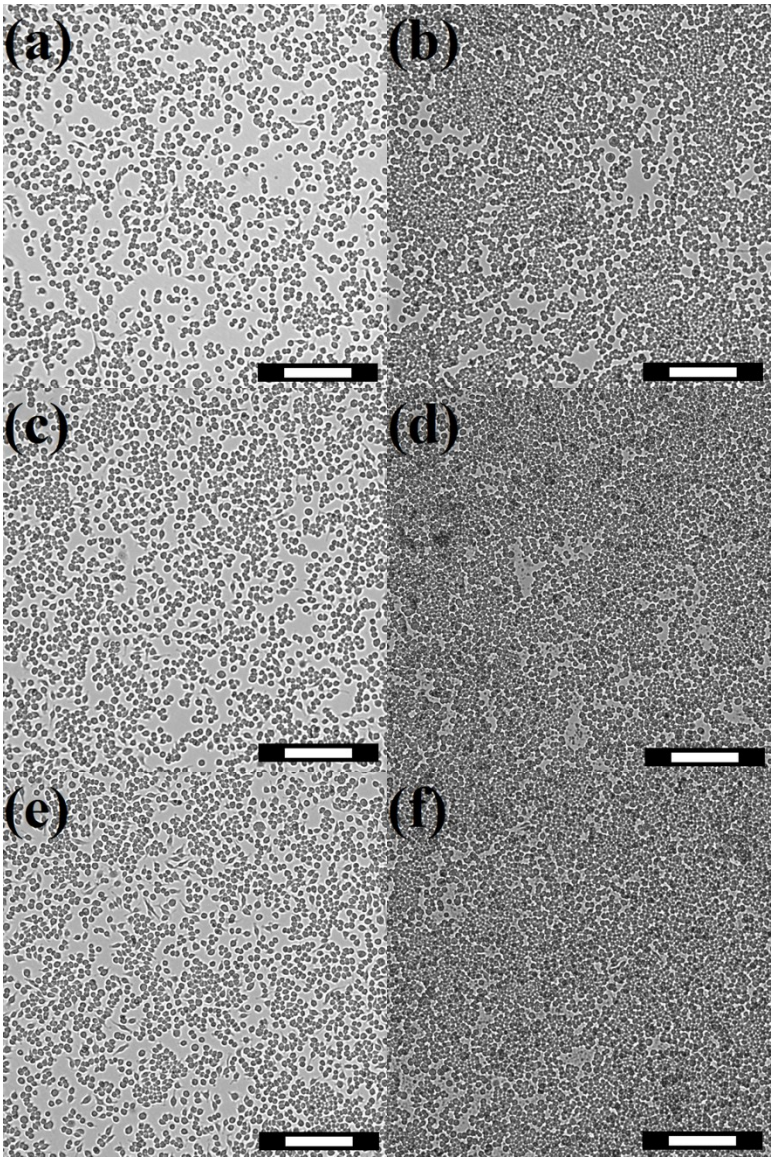

Fig. S6 Addition of $LaPO_4$ C and C2S NPs did not alter RAW 264.7 cell growth. Brightfield images of RAW 264.7 macrophage cells (a) before and (b) 24 h after incubation; and with 29.2 μg/mL of $LaPO_4$ (c, d) C and (e, f) C2S NPs. Scale bar: 200 μm.

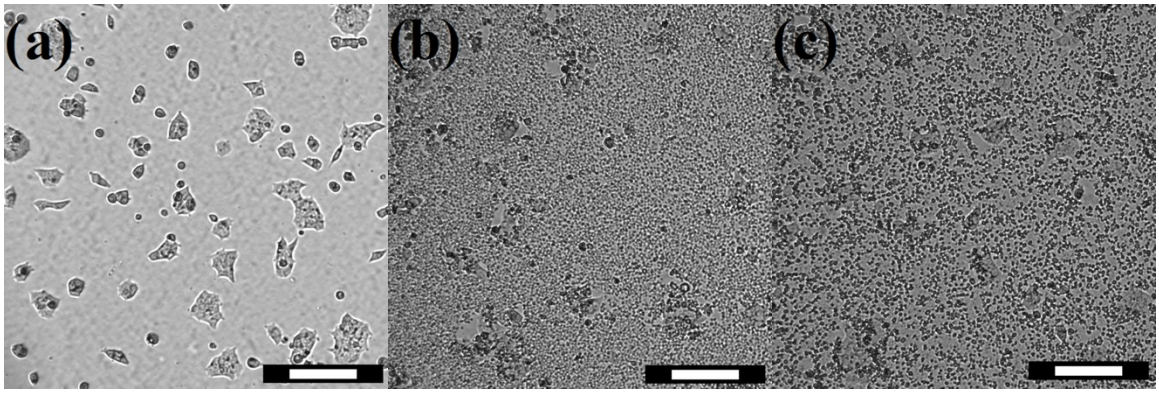

Fig. S7 $LaPO_4$ C and C2S NPs precipitate over BT-474 cells. Brightfield images of BT-474 breast cancer cells after 24 h of incubation (a) in the absence of NPs, (b) with 29.2 µg/mL of $LaPO_4$ C NPs, and (c) with 29.2 µg/mL of C2S NPs. Scale bar: 200 µm.

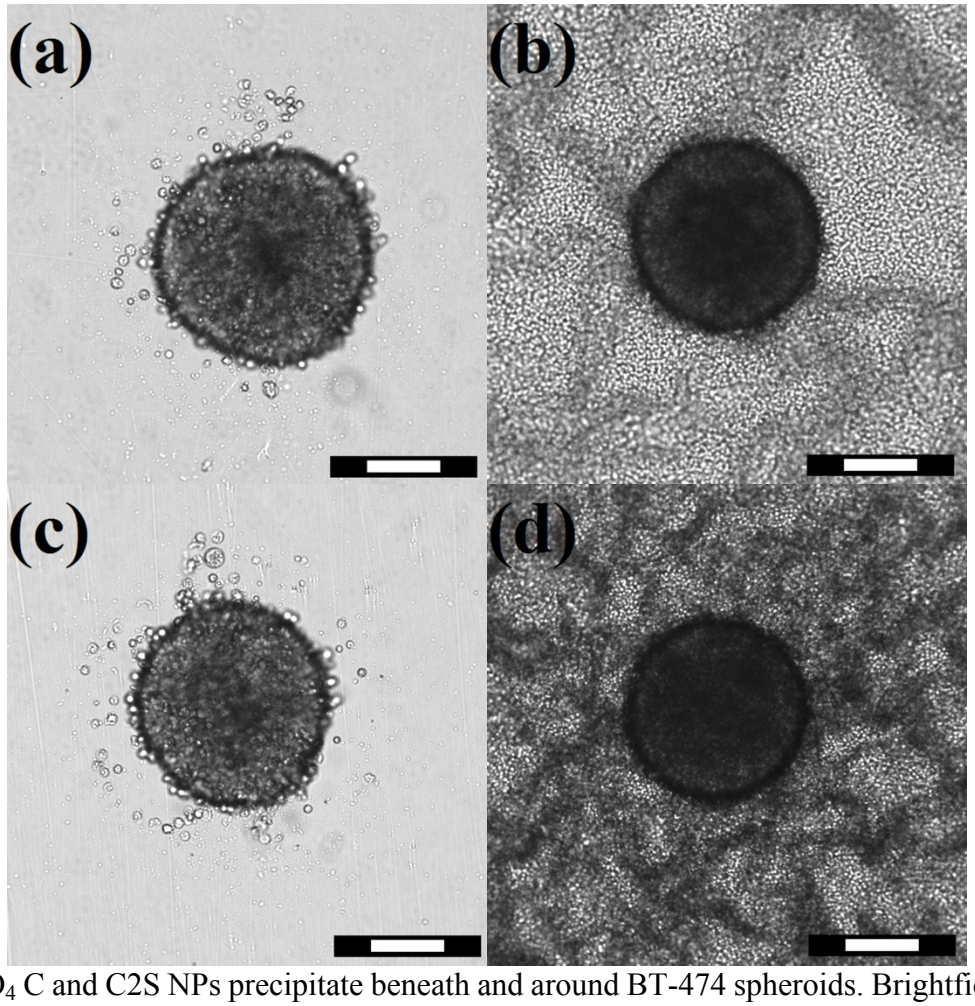

Fig. S8 $LaPO_4$ C and C2S NPs precipitate beneath and around BT-474 spheroids. Brightfield images of BT-474 spheroids before and after incubation for 24 h with 116.9 µg/mL of $LaPO_4$ (a, b) C and (c, d) C2S NPs. Scale bar: 200 µm.